

引用格式：王冠民，祝新怡，刘海，等，2024. 沉积微相在致密砂岩可压裂性分析中的应用：以鄂尔多斯盆地陇东地区延长组 7 段为例[J]. 地质力学学报, 30 (6) : 893–905. DOI: [10.12090/j.issn.1006-6616.2024004](https://doi.org/10.12090/j.issn.1006-6616.2024004)

Citation: WANG G M, ZHU X Y, LIU H, et al., 2024. The application of sedimentary microfacies on the fracability of tight sandstone reservoir in Chang 7 member of Longdong area in the Ordos Basin[J]. Journal of Geomechanics, 30 (6) : 893–905. DOI: [10.12090/j.issn.1006-6616.2024004](https://doi.org/10.12090/j.issn.1006-6616.2024004)

## 沉积微相在致密砂岩可压裂性分析中的应用——以鄂尔多斯盆地陇东地区延长组 7 段为例

王冠民<sup>1</sup>, 祝新怡<sup>1</sup>, 刘海<sup>2</sup>, 陈帅<sup>3</sup>, 石晓明<sup>1</sup>, 胡津<sup>1</sup>

WANG Guanmin<sup>1</sup>, ZHU Xinyi<sup>1</sup>, LIU Hai<sup>2</sup>, CHEN Shuai<sup>3</sup>, SHI Xiaoming<sup>1</sup>, HU Jin<sup>1</sup>

1. 中国石油大学（华东）地球科学与技术学院，山东 青岛 266580;

2. 川庆钻探工程有限公司长庆井下技术作业公司，陕西 西安 710018;

3. 中国电建集团北京勘测设计研究院有限公司，北京 100024

1. School of Geosciences, China University of Petroleum (East China), Qingdao 266580, Shandong, China;

2. Changqing Underground Technology Operation Company of Chuanqing Drilling Engineering Co., Ltd., Xi'an 710018, Shaanxi, China;

3. Beijing Engineering Corporation Limited, Beijing 100024, China

### The application of sedimentary microfacies on the fracability of tight sandstone reservoir in Chang 7 member of Longdong area in the Ordos Basin

**Abstract:** [Objective] Sedimentary differences are the key factor in controlling reservoir heterogeneity. Analyzing reservoir heterogeneity through sedimentary microfacies is crucial for oil and gas field development and sweet spot prediction, and it also informs the evaluation of fracturing in tight sandstone reservoirs. There are many types and complex lithologies of unconventional oil and gas reservoirs in the Ordos Basin as well as many factors controlling reservoir fracability. At present, mechanical experiments are used to comprehensively characterize the fracturing property; however the research cost is high and the experimental process is complicated, making it unsuitable for large-scale oilfield development and use. Therefore, this study attempted to analyze and compare the fracability of tight sandstones with different sedimentary microfacies from the perspective of sedimentary microfacies controlling the lithology and reservoir development to provide a reference for oilfield development plans. [Methods] Taking the compact sandstone of Chang 7 member of Yanchang Formation in the Longdong area of Ordos Basin as the research object, the different types of microfacies are identified through the data of core and cast slice, the mineral composition and structural parameters of rock samples were obtained by X-ray diffraction (XRD) analysis, and rock mechanics experiments were conducted to quantitatively described the fracturing property. [Results] The results are as follows: (1) Two sedimentary microfacies, namely underwater distributary channel and sheet sand, mainly developed in Chang 7 Member of Yanchang Formation in the study area. Among them, the single sand body thickness of the underwater distributary channel is greater than 2 m, the sheet sand is mostly a medium thin and thick sand mudstone interlayer, and the single sand body thickness is generally less than 2 m. (2) The composition and structure of the two sedimentary sandstone microfacies are obviously different: the content of carbonate minerals, clay minerals, and heterobases in the sheet sand microfacies are relatively high, the particle size is finer, and the sorting is worse, which are the main internal factors that cause the difference in tight sandstone fracability and are the basis for judging the fracability of tight sandstone by sedimentary microfacies. (3) The fracability index was related to the composition and structure of sandstone. In terms of composition, the fracability index was

基金项目：国家自然科学基金项目（41972131）

This research is financially supported by the National Natural Science Foundation of China (Grant No. 41972131).

第一作者：王冠民（1969—），男，博士，教授，研究方向为沉积学与储层地质学。Email: [wangguanmin@upc.edu.cn](mailto:wangguanmin@upc.edu.cn)

收稿日期：2023-12-01；修回日期：2024-01-15；录用日期：2024-07-11；网络出版日期：2024-11-11；责任编辑：范二平

positively correlated with quartz mineral content as well as carbonate mineral content and negatively correlated with feldspar mineral content. In terms of structure, there is a negative correlation between the fracability index and the average particle diameter  $\varphi$ . The larger the particle size, the higher the fracability index. The fracability index was positively correlated with the standard deviation of the particle size, indicating that the worse the particle separation, the higher the fracability index. (4) Through grey correlation analysis, it was found that the degree of influence of sandstone parameters on fracability was in the order of carbonate mineral content, quartz content, standard deviation of particle size, and average particle size from high to low, while clay minerals and feldspar content were in a relatively weak position. [Conclusion] The results indicate that the higher the contents of carbonate and quartz and the higher the standard deviation of particle size (the worse the sorting), the better the fracability. The finer the particle size, the higher the feldspar content and the worse the fracability. Grey correlation analysis showed that the carbonate mineral content, separation and particle size play a major role in the fracability of tight sandstone. Compared with distributary channel microfacies, sheet sand has a higher carbonate minerals content, worse sorting, and little difference in quartz content. Although the microphase particle size of the sheet sand is slightly finer, the average particle size has a relatively minor effect on the fracability; thus, sheet sand as a whole shows better fracability. [Significance] Since the standard deviation (sorting) and particle size of sandstone particles are controlled by sedimentary microfacies, and the content of carbonate minerals is directly controlled by sandstone thickness and indirectly affected by sedimentary microfacies, the change in the tight sandstone fracability index can be judged according to the difference in sedimentary microfacies in practical engineering, and the working process can be simplified.

**Keywords:** Yanchang Formation; tight sandstone; fracability; sedimentary microfacies; distributary channel; sheet sand

**摘要：**沉积特征差异是控制储层非均质性的关键因素之一，利用沉积微相来分析储层的非均质性通常是油气田开发和储层甜点预测的重要手段，也可以尝试用其评价致密砂岩储层的可压裂性。以鄂尔多斯盆地陇东地区延长组7段（长7段）的致密砂岩为研究对象，在通过岩芯、测井等资料识别不同沉积微相类型基础上，利用全岩X射线衍射（XRD）分析、铸体薄片观察得到致密砂岩样品的矿物成分和结构参数，并结合岩石力学实验，采用脆性指数和三轴抗压强度的比值来表征岩石的可压裂性。将致密砂岩的沉积微相、成分结构和可压裂性进行对比分析后得到以下认识：长7段致密砂岩主要发育水下分流河道和席状砂2种沉积微相，不同沉积微相之间的矿物成分、结构存在明显差异；与席状砂相比，水下分流河道砂体的平均粒径更大，分选更好，碳酸盐矿物和黏土矿物含量更低，杂基含量更少；可压裂性指数与砂岩的石英含量、碳酸盐矿物含量、粒度分布标准偏差具有正相关性，与长石含量、平均粒径具有负相关性。灰色关联分析表明碳酸盐矿物含量、粒度分布标准偏差、粒径是影响长7段致密砂岩可压裂性的最主要因素，整体上席状砂的可压裂性指数要高于水下分流河道砂，更易于压裂。由于砂岩颗粒的粒度分布标准偏差、粒径受沉积微相控制，碳酸盐矿物含量受砂岩厚度直接控制、受沉积微相间接控制，故在致密砂岩油气储层压裂的实际工程中可以依据沉积微相差异来判断致密砂岩的可压裂性变化，简化可压裂性的评价流程。

**关键词：**延长组；致密砂岩；可压裂性；沉积微相；水下分流河道；席状砂

中图分类号：TE121 文献标识码：A 文章编号：1006-6616(2024)06-0893-13

DOI: [10.12090/j.issn.1006-6616.2024004](https://doi.org/10.12090/j.issn.1006-6616.2024004)

## 0 引言

目前全球油气勘探开发已进入常规油气稳定上产、非常规油气快速发展阶段（[刘联群等, 2010](#)；[姚泾利等, 2013](#)；[张海林等, 2014](#)）。对于大多数非常规油气藏来说，压裂是其主要的开发手段。开发实践表明，非常规储层普遍依靠水力压裂，储层的可

压裂性是评价致密油开发甜点的一项重要指标（[邹才能等, 2014](#)；[杨帆等, 2023](#)）。鄂尔多斯盆地的非常规油气储层类型多、岩性复杂，储层可压裂性的控制因素也较多，如何快速分析不同砂岩的可压裂性是非常规油气储层开发工作的难点之一。

目前致密砂岩可压裂性多从岩石力学、矿物成分、脆性等方面进行研究，并取得了一系列进展。[Sui et al. \(2016\)](#)基于层次分析法，综合考虑岩石的脆

性、脆性矿物含量、黏土矿物含量、黏聚力、内摩擦角和无侧限抗压强度等参数对可压裂性的影响,定量评估了岩石的可压裂性,认为裂缝越复杂,可压裂性越好;Wu et al.(2018)利用扫描电镜(SEM)观察,评价储层脆性、矿物含量、成岩作用和天然裂缝对可压裂性的影响,对岩石进行了可压裂性的评估,认为脆性矿物含量大、热演化程度高、裂缝发育良好是压裂的有利条件;He et al.(2019)等基于层次分析法,提出了综合力学脆性、无侧限抗压强度、矿物脆性、内聚力、内摩擦角、天然裂缝、断裂韧性、水平应力差和断裂屏障等因素的可压裂性评价模型,认为天然裂缝、机械脆性、矿物脆性对可压裂性的影响更大;刘建等(2021)建立三维力学模型进行数值模拟,认为鄂尔多斯盆地含水地区长6段致密砂岩储层的岩石力学性质影响了现今地应力分布,进而导致了可压裂性的不同;赵进雍等(2022)结合三轴岩石力学实验和三维力学反演方法,对准噶尔盆地四棵树凹陷侏罗系—白垩系储层分析,认为岩石力学参数受岩性变化控制,岩石粒度越粗,杨氏模量越大、泊松比越小,越容易形成裂缝。除了分析致密砂岩的可压裂性以外,对于储层裂缝发育程度、裂缝网络形成机理的研究也成为了关注重点。李年银等(2016)利用裂缝网络形成机理,结合储层可压裂性和天然裂缝的发育程度等方面,认为岩石脆性越大,断裂韧性越小,越有利于裂缝扩展延伸;慕立俊等(2019)从水力裂缝扩展规律及裂缝形态综合认识评价入手,认为岩石中复杂网络形成的先决条件是具备较高的脆性指数。

尽管通过力学实验获取多种参数来综合表征可压裂性的方法比较准确,但力学实验的研究成本较高且实验流程繁琐,不适合油田的大规模开发利用。相对而言,沉积相和岩相的变化更容易识别,且砂砾岩的成分、结构等岩性因素主要受控于沉积作用,所以从岩相或沉积相变化来判断致密砂岩的可压裂性,在实际工作中更有应用意义。故以鄂尔多斯盆地陇东地区延长组7段(长7段)致密砂岩储层为例,尝试从沉积微相控制岩性和储层发育的角度,分析和对比不同沉积微相致密砂岩的可压裂性,为油田开发方案提供参考。

## 1 研究区地质特征

## 1.1 地质背景

鄂尔多斯盆地位于华北地台西部，是一个中生

代与新生代叠加的、有多期次旋回且沉降稳定的大型坳陷盆地(李相博等, 2010)。伊陕斜坡是鄂尔多斯盆地内部的一个大型次级构造带, 其边缘断裂褶皱发育, 区内地形平缓, 内部构造相对简单, 表现为由东向西倾斜的大型平缓单斜, 局部发育低幅度的鼻状构造, 是中国致密油勘探开发的核心区(姚泾利等, 2013; 张海林等, 2014; 孙越等, 2022)。研究区所涉及的陇东地区位于伊陕斜坡的西南部, 具体位置如图1所示。

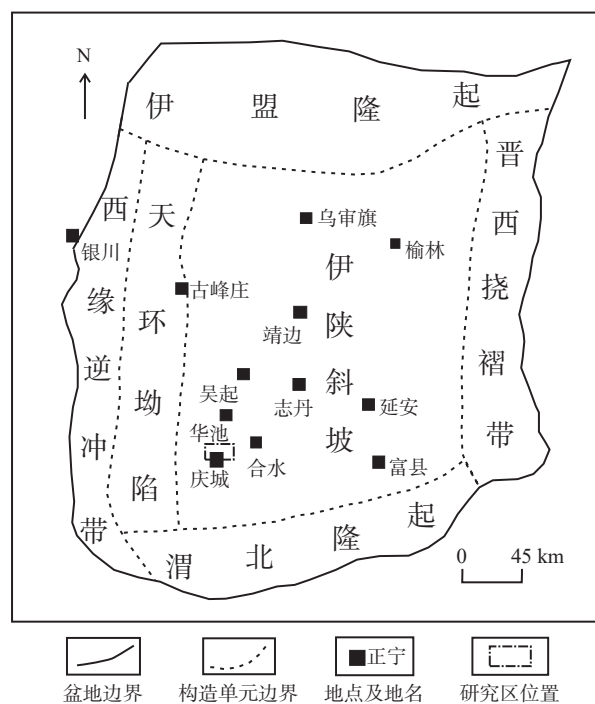


图 1 研究区具体位置

Fig. 1 Location map of the study area

陇东地区长7段是一套湖泊—三角洲沉积的细碎屑岩(曹跃等, 2018), 整体上为砂泥岩互层, 厚度上南厚北薄, 粒度上南细北粗。长7段发育的三角洲前缘砂体是油气的主要储集岩, 具有储层致密、连通性差、非均质性强的特点(张哲豪等, 2020)。根据区域标志层并结合沉积旋回, 延长组可细分为10个段(表1), 其中长7段可分为3个亚段。

## 1.2 储层的岩石学特征

研究区长7段的致密砂岩主要为灰色长石岩屑细砂岩。根据XRD全岩分析,矿物成分包括石英、钾长石、斜长石、白云石、铁白云石、黏土矿物以及少量的方解石、菱铁矿等。为了方便后续研究,将矿物类型归纳为石英、长石(包括钾长石、斜长石)、碳酸盐矿物(包括方解石、白云石、铁白云

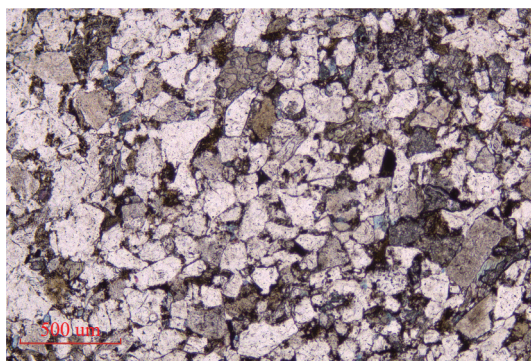
表 1 陇东地区延长组地层划分及岩性特征

Table 1 Stratigraphic division and lithological characteristics of the Yanchang Formation in the Longdong region

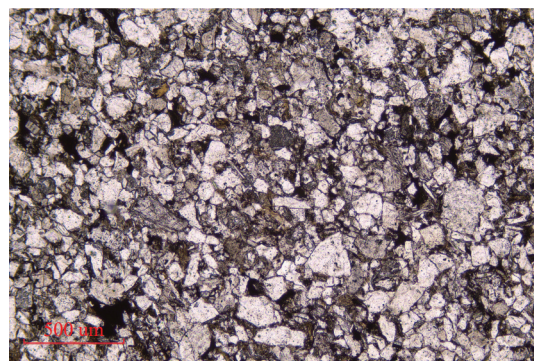
地层时代			地层岩性
统	组	段	
上三叠统	延长组	1	深灰色泥、页岩夹煤层, 局部为厚层块砂
		2	灰绿色中—细砂岩夹灰色—深灰色泥岩、黑褐色炭质泥岩
		3	
		4+5	
		6	深灰色—灰黑色泥、页岩与灰色—灰绿色粉砂岩互层, 下部发育一套油页岩、泥岩夹薄层凝灰岩
		7	
		8	深灰色—灰黑色泥岩与浅灰绿色—褐灰色中—细砂岩互层
		9	
		10	灰绿色厚层块中—粗长石砂岩夹深灰色及暗紫色泥岩

石、菱铁矿)、黏土矿物 4 大类。其中, 石英含量为 50%~63%, 平均为 55.2%; 长石含量为 18%~26%, 平均为 23.1%; 碳酸盐矿物含量为 9%~20%, 平均为 11.4%; 黏土矿物含量为 5%~10%, 平均为 7.1%。

根据镜下薄片观察, 研究区长 7 段的砂岩以细砂为主, 分选中等—较好, 颗粒磨圆程度中等, 次棱角状—次圆状, 颗粒支撑, 颗粒之间以线接触、孔隙式胶结为主(图 2)。



(a) 中砂岩水下分流河道微相, 分选较好, 次棱角状, Y24 井 2150.7 m, 单偏光



(b) 细砂岩席状砂微相, 分选偏差, 次棱角状, Y24 井 2141.6 m, 单偏光

图 2 不同沉积微相砂岩样品的显微镜下特征

Fig. 2 The characteristics of different sandstone microfacies under the microscope

(a) Underwater distributary channel microfacies of sandstone, with good sorting, sub-angular, well Y24 at 2150.7 m, under monochromatic polarized light; (b) Sheet sand microfacies of fine sandstone, poor sorting, sub-angular, well Y24 at 2141.6 m, under monochromatic polarized light

## 2 长 7 段沉积微相特征与差异性分析

迄今为止, 很多学者认为鄂尔多斯盆地陇东地区长 7 段存在重力流沉积: 浊流或砂质碎屑流(杨华等, 2010; 廖纪佳等, 2013; 付金华等, 2015; 刘芬等, 2015; 张晓辉等, 2020)。也有部分学者持不同看法, 邹才能等(2009)认为陇东地区长 7 段的致密储层主要为三角洲前缘砂岩和重力流砂岩, 李兆扬等

(2012)认为陇东地区延长组长 7 段主要由湖泊和三角洲沉积体系组成。

通过研究区长 7 段岩芯的仔细分析, 认为长 7 段的沉积亚相主要为三角洲前缘亚相而非重力流, 主要依据如下: ① 岩心中可见流水交错层理(图 3a), 该类型层理难以出现在重力流沉积中, 应该代表河道沉积; ② 岩心发育脉状层理(图 3b), 这也是无法用重力流沉积解释的, 应属于水下天然堤、席状砂沉积构造; ③ 岩芯中可见密集的碳屑纹

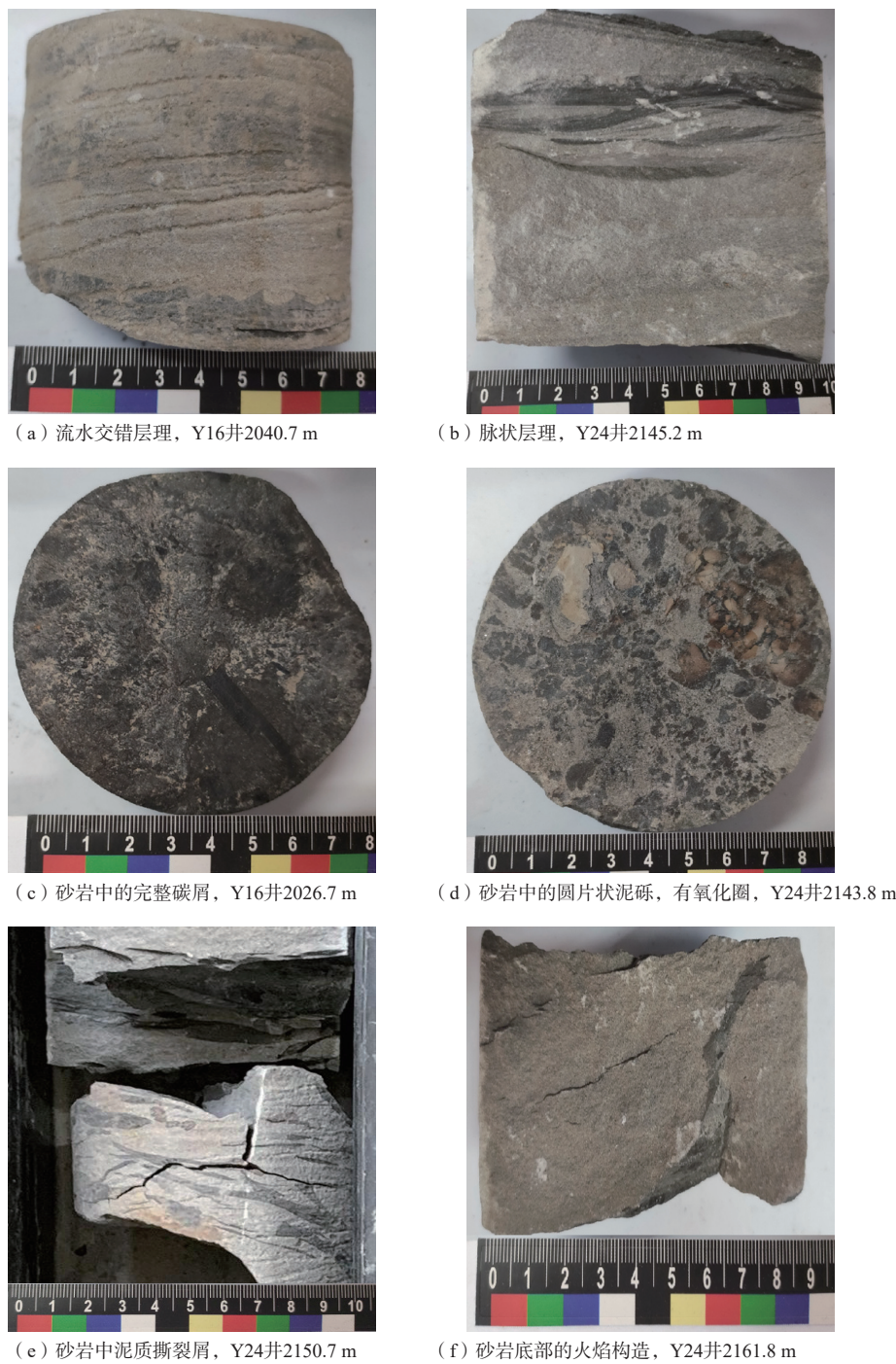


图3 岩芯中典型的沉积相标志

Fig. 3 Typical sedimentary phenomena in rock cores

(a) Fluvial cross-bedding, well Y16 at 2040.7 m; (b) Flaser bedding, well Y24 at 2145.2 m; (c) Intact carbon debris in sandstone, well Y16 at 2026.7 m; (d) Disc-shaped mud chips in sandstone with oxidation halo, well Y24 at 2143.8 m; (e) Muddy rip-up clasts in sandstone, well Y24 at 2150.7 m; (f) Flame structure at the base of sandstone, well Y24 at 2161.8 m

层(图3c),部分碳屑较完整,代表缓慢的近岸浅水沉积,在重力流沉积中难以出现;④岩心中常见河底短距离搬运、沉积形成的泥砾(图3d),扁平、磨圆好,甚至发育氧化圈;⑤泥质撕裂屑(图3e)不仅仅见于重力流滑塌,也是河流环境常见的现象;

⑥所有砂泥岩界面处的变形,都是差异压实作用形成的,典型的有重荷模构造、火焰构造(图3f);⑦未见滑塌变形、粒序层理等重力流沉积构造。

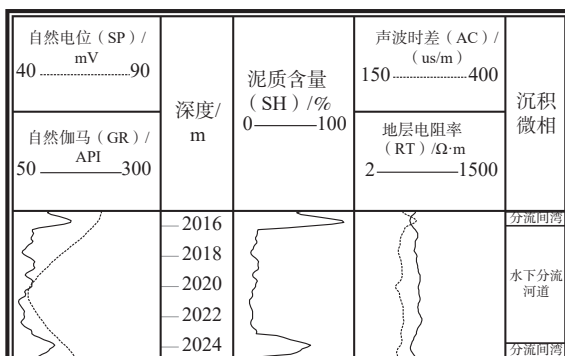
## 2.1 沉积微相类型划分

通过岩芯识别及测井资料分析,研究区长7段

与致密砂岩有关的沉积微相主要有水下分流河道与席状砂2种。

### 2.1.1 水下分流河道

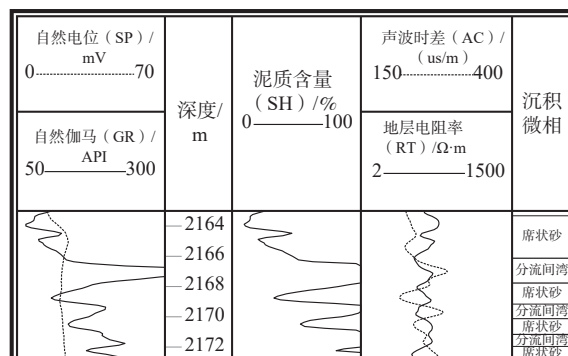
从岩芯上来看,水下分流河道的单层砂体厚度一般大于2 m,分选中等一好,杂质含量一般低于10%,沉积构造以平行层理为主,可见槽状交错层理,底部具冲刷面。水下分流河道砂体在纵向上缺乏典型曲流河的正旋回,表明水下分流河道沉积缺乏明显的侧向迁移,这符合浅水三角洲的沉积背景。从测井资料来看,自然伽马(GR)曲线形态呈光滑或微齿化的箱形(图4a)。



(a) 水下分流河道的测井曲线形态, Y16井

### 2.1.2 席状砂

席状砂是围绕浅水三角洲分流河道砂体周围展布的相对偏薄砂体,包括分流河道末端因河道消失而散开沉积的砂体,以及河道两侧因决口、溢岸而沉积的砂体。从岩芯上看,单层席状砂的厚度一般小于2 m,主要表现为中厚层砂岩夹泥岩,或者与泥岩互层。席状砂的分选较差(图2b),杂质含量接近15%。沉积构造以砂纹层理、平行层理为主,可见碳屑纹层。在测井曲线上,GR曲线形态呈低一中幅指形,偶见漏斗形和钟形,齿化现象明显(图4b)。



(b) 席状砂的测井曲线形态, Y24井

图4 水下分流河道和席状砂微相的测井曲线特征

Fig. 4 Logging curve characteristics of underwater distributary channels and sheet-like sand microfacies

(a) The logging curve morphology of underwater distributary channels, Y16 well; (b) The logging curve morphology of sheet sand, Y24 well

## 2.2 不同沉积微相砂岩的成分差异

基于研究区长7段岩芯样品的全岩XRD结果,把水下分流河道与席状砂微相砂岩、长石、碳酸盐矿物和黏土矿物4种成分的含量进行了对比(图5)。

结果表明,水下分流河道砂岩中石英含量主要分布在56%~64%,席状砂的石英含量处于48%~64%(图5a);水下分流河道砂岩中长石含量主要分布在21%~27%,而席状砂的长石含量主要分布在15%~21%,水下分流河道砂岩的长石含量相对较高(图5b);水下分流河道砂岩中碳酸盐矿物含量分布在7%~13%,席状砂的碳酸盐矿物含量的分布范围比分流河道广,分布在7%~19%,且多数集中于16%~19%,席状砂的碳酸盐矿物含量相对更高(图5c);水下分流河道砂岩中黏土矿物含量分布在3%~9%,席状砂的黏土矿物含量分布在7%~11%(图5d),水下分流河道砂岩的黏土矿物含量整体小于席状砂。

席状砂与水下分流河道砂的成分相比,整体具有低长石含量、高碳酸盐矿物含量、高黏土矿物含

量的特点。其中,席状砂的碳酸盐矿物偏高,是因为源于暗色泥岩的富碳酸盐成岩流体进入砂岩后,在偏薄的席状砂中可以占据更大比例的胶结空间,席状砂中偏高的碳酸盐胶结物含量又降低了长石与石英的相对含量。

## 2.3 不同沉积微相砂岩的结构差异

在结构方面,分流河道砂岩的平均粒径多分布在2.8~3.0 $\phi$ ,席状砂平均粒径多分布在3.0~3.2 $\phi$ ,水下分流河道砂岩比席状砂微相的粒度更粗(图6a)。水下分流河道砂岩的粒度分布标准偏差主要分布于0.5~0.7,而席状砂的粒度分布标准偏差多分布在0.6~0.7,故水下分流河道砂岩的分选更好(图6b),粒度相对更粗(图6)。

## 3 可压裂性表征方法

### 3.1 岩石力学实验

研究区样品的岩石力学参数是通过岩石常规

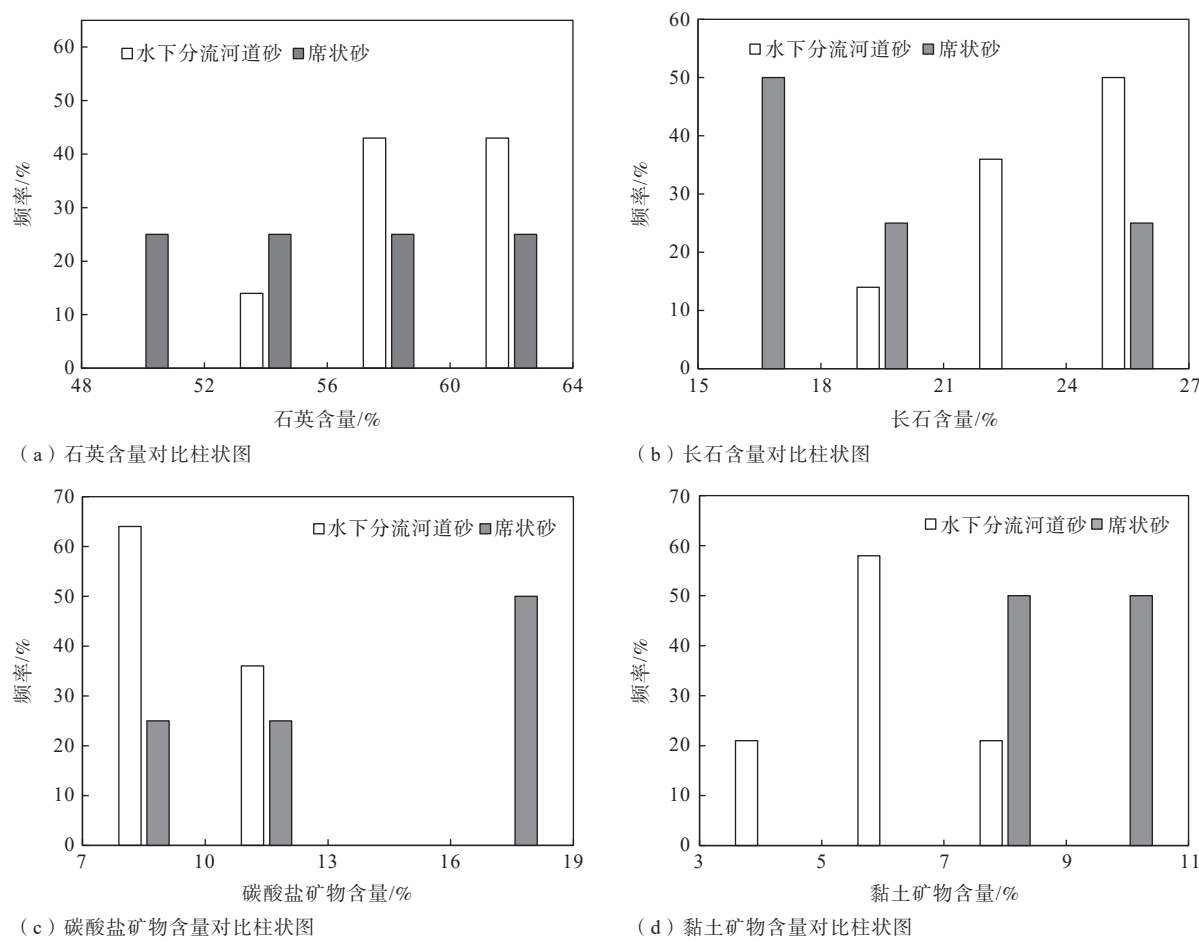


图5 不同沉积微相砂岩的矿物成分对比

Fig. 5 Comparison of mineral composition of sandstones with different sedimentary microfacies

(a) Quartz content comparison bar chart; (b) Feldspar content comparison bar chart; (c) Carbonate minerals content comparison bar chart  
Clay mineral content comparison bar chart

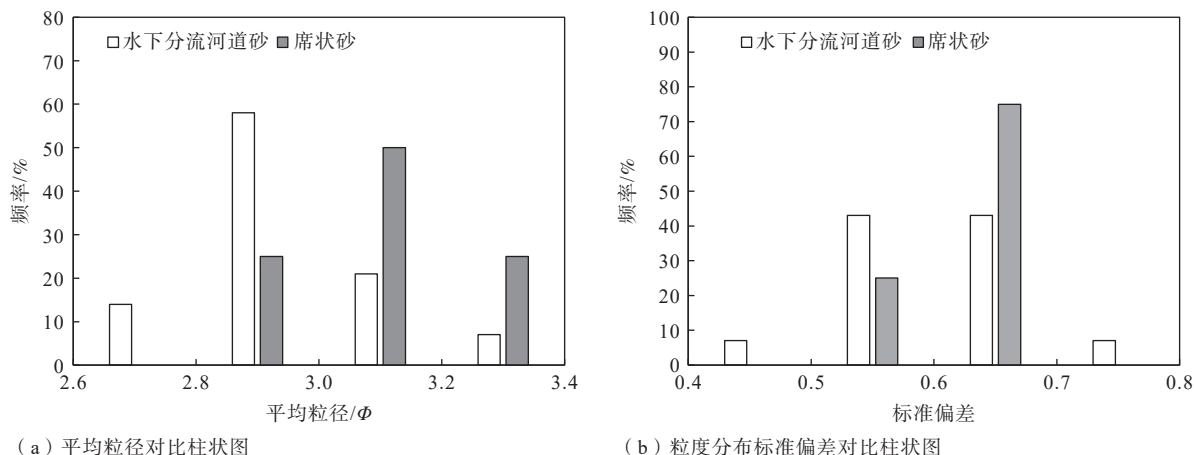


图6 不同沉积微相砂岩的结构对比

Fig. 6 Comparison of sandstone structures between different sedimentary microfacies

(a) Average particle size comparison bar chart; (b) Particle size distribution standard deviation comparison bar chart

三轴实验测量所得, 使用全伺服控制三轴测试系统 (TAW-1000) 进行一系列应力-应变测试, 得到样品

的弹性模量、泊松比和抗压强度, 具体实验过程如下。

(1) 将岩石试件切割打磨至标准尺寸(直径×高

度)25 mm×50 mm;

(2)将试件用密封套包住,放置在压力室,通过增压器对试样提供一定围压(模拟地层压力),待围压稳定后通过轴向加载系统对试件进行宏观破坏;

(3)依据实验仪器自动记录岩石破坏载荷、轴向变形量和径向变形量可以计算得出所需要的岩石力学参数,如公式(1)(2):

$$E = \Delta\sigma_h / \Delta\varepsilon_h \quad (1)$$

$$\mu = \Delta\varepsilon_v / \Delta\varepsilon_h \quad (2)$$

式中: $E$ 为弹性模量; $\mu$ 为泊松比; $\Delta\sigma_h$ 为弹性变形阶段内任意两点的轴向应力变化量; $\Delta\varepsilon_h$ 为弹性变形阶段内对应两点的轴向应变变化量; $\Delta\varepsilon_v$ 为弹性变形阶段内对应两点的轴向径向应变变化量。

### 3.2 可压裂性表征

可压裂性指数是一个后续引出的术语,常被用来评价油气藏储层的可压裂程度(Kivi et al., 2018)。近年来,已经提出了许多用于评估非常规油气藏可压裂性的量化方法(袁俊亮等,2013; Wang et al., 2015; Fu et al., 2015; Wu et al., 2018)。在这些方法中,计算可压裂性的参数包括脆性指数、断裂韧性、抗压强度、天然裂缝密度、不同的水平应力等。其中,被大家广泛认可的是脆性指数。尽管脆性指数的表示方法有多种,但国内大多数学者采用由Rickman et al.(2008)根据弹性模量和泊松比求得的岩石力学参数法。同时,大部分学者也认为仅使用脆性指数来衡量岩石的可压裂性是不够的(Jin et al., 2015; Holt et al., 2015; Bai, 2016; Kivi et al., 2018)。

除了脆性指数外,目前还较多地采用断裂韧性来计算可压裂性。不过,断裂韧性是一个有待商榷的参数,其争议性主要在于2点:①断裂韧性的实验方法较多且计算结果各不相同(Fowell, 1995; Wang et al., 1998; 贾学明和王启智, 2003; 樊鸿等, 2011),目前尚没有一种实验方法被广泛认可。②断裂韧性的概念比脆性指数要广且存在一定的交集。断裂韧性与材料断裂前吸收的能量或外界对材料所做的功的大小密切相关,其相对大小可以用应力-应变曲线下的面积来间接表示(李进步等, 2015),而脆性指数反映的仅是岩石承受外力作用的应变特性。考虑到断裂韧性的争议性,文中未采用其表征可压裂性。

考虑到岩石受压破裂过程和应力-应变之间的密切相关性以及岩石在地下的围压环境,文中引入

与应力相关的参数——三轴抗压强度来表征可压裂性。三轴抗压强度是三向压力作用下发生宏观破裂时岩石承受的最大轴向压应力,反映的是岩石受力破坏时的应力情况。岩石的承压能力越强,岩石越难以被破坏。

基于岩石本构关系,采用脆性指数和三轴抗压强度的比值来表征岩石的可压裂性,表征公式如下:

$$F_{rac} = B / \sigma; \quad (3)$$

式中: $F_{rac}$ 为可压裂性指数; $B$ 为根据Rickman et al.(2008)的岩石力学参数法求得的脆性指数; $\sigma$ 为三轴抗压强度。

## 4 可压裂性与砂岩成分、结构的关系

根据上述实验与表征方法,文中对研究区长7段的18块致密砂岩储层样品进行了力学测试,计算其可压裂性指数,并进一步分析可压裂性指数与砂岩成分、结构变化的关系。

### 4.1 可压裂性与砂岩成分的关系

根据研究区长7段的全岩XRD结果,致密砂岩样品中的矿物组分主要包括石英、长石、碳酸盐矿物以及黏土矿物4大类。砂岩可压裂性与各种矿物成分的相关性如下图所示(图7)。

砂岩的可压裂性与石英含量呈较好的正相关关系(图7a),石英硬度较大,在致密砂岩中可作为脆性矿物的代表,石英矿物的存在增大了微裂缝的延伸距离,使得致密砂岩的裂缝网络更为发育,增大了岩石的可压裂性。砂岩的可压裂性与长石含量表现为负相关关系(图7b),主要原因是砂岩中的长石普遍发生蚀变使得长石的力学性质发生了变化,蚀变生成更多的黏土矿物导致砂岩整体可压裂性降低。砂岩的可压裂性与碳酸盐矿物含量呈正相关关系(图7c),碳酸盐矿物作为脆性矿物(Estupiñan et al., 2007; 钟大康等, 2007),含量的增加有利于提高岩石的可压裂性。砂岩的可压裂性与黏土矿物含量的相关性较差(图7d),原因包括2个方面:①黏土矿物含量相较其他矿物含量偏少,其对可压裂性的影响被其他高含量矿物的影响所掩盖;②黏土矿物的存在形式较多,主要有长石蚀变形成的黏土矿物、泥质杂基以及泥屑,这些因素综合作用导致黏土矿物与砂岩可压裂性的相关性偏低。

### 4.2 可压裂性与砂岩结构的关系

文章通过Image-Pro Plus 6.0软件对砂岩薄片进

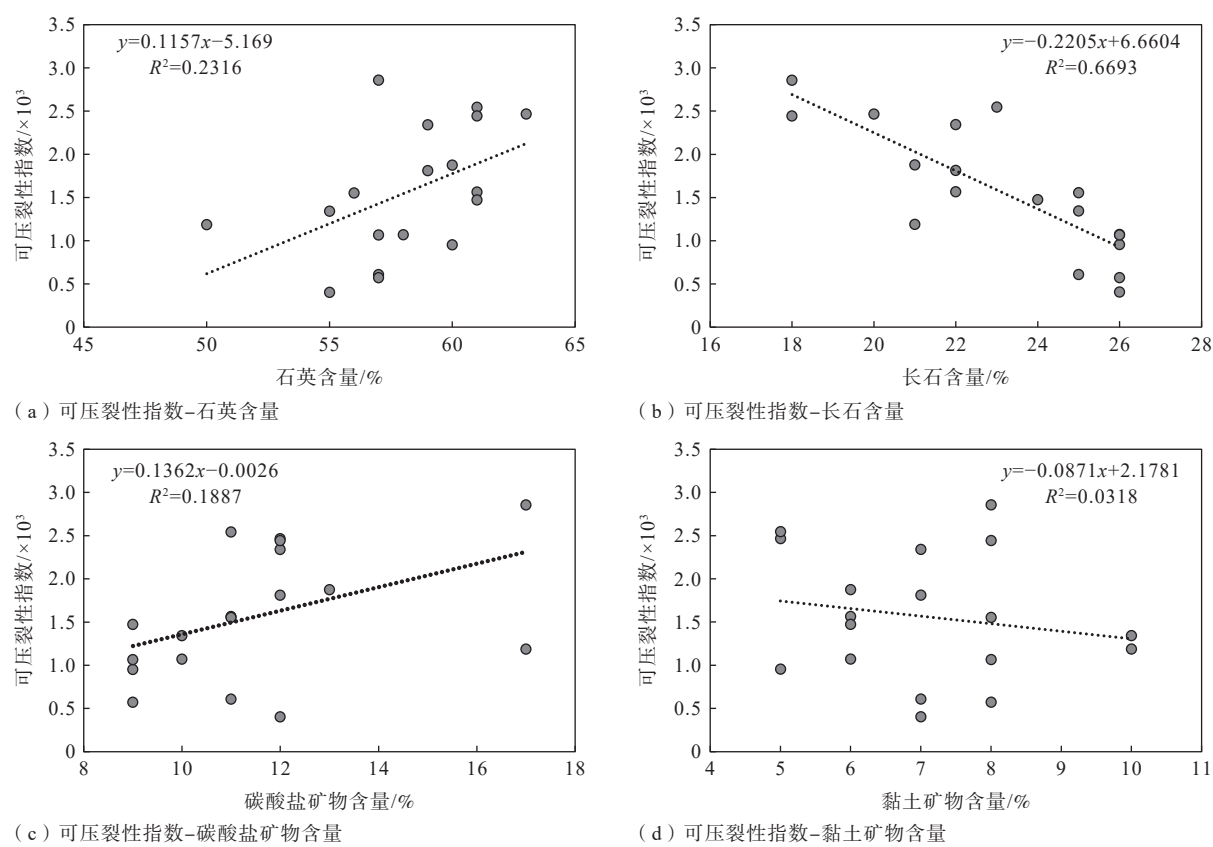


图 7 砂岩各种矿物成分与可压裂性之间的关系

Fig. 7 The correlation between mineral composition and fracturing ability

(a) Fracability index-quartz content; (b) Fracability index-feldspar content; (c) Fracability index-carbonate mineral content; (d) Fracability index-clay mineral content

行图像粒度分析, 来确定砂岩样品的结构参数。使用 Friedman 矩法(Frankie, 2016)计算岩石样品的颗

粒平均粒径和标准偏差。砂岩的可压裂性与砂岩结构的具体相关性如下图(图 8)所示。

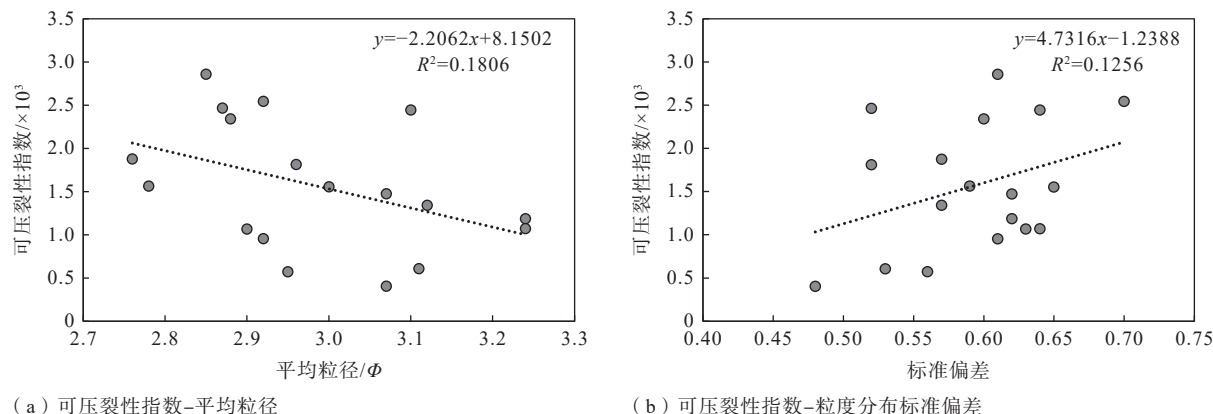


图 8 砂岩结构与可压裂性之间的关系

Fig. 8 The relationship between sandstone structure and fracturing ability

(a) Fracability index-average particle size; (b) Fracability index-grain size distribution standard deviation

研究区长 7 段砂岩的颗粒平均粒径与可压裂性指数表现出一定的负相关关系(图 8a)。由于裂缝的延伸过程遵循最小耗能原理(Tang et al., 2008),

由格里菲斯能量准则可知, 在脆性颗粒中裂纹扩展单位面积所需要的能量远小于裂纹在塑性物质中扩展单位面积所消耗的能量, 因而裂纹在脆性颗粒

内部传播比在颗粒周围的塑性物质中传播会消耗更少能量。在相同区域面积内,脆性矿物颗粒的粒径越大,微裂缝传播消耗的能量越少。因此随着砂岩平均粒径增大,可压裂性指数不断降低。

随着粒度分布标准偏差的增大,可压裂性指数随之增大,呈现正相关的趋势(图8b)。标准偏差越大,分选越差,杂基越多,理论上裂缝扩展阻力越大,裂纹扩展时提供的能量释放率也就越大。但实际上由于砂岩颗粒与杂基之间的结合力最弱,故当砂岩中的杂基含量适当增高后,裂缝可以更多经过颗粒边缘延伸,导致裂缝的延伸距离更远,可压裂性反而可能变好。

## 5 沉积微相差异对砂岩可压裂性的影响分析

### 5.1 不同沉积微相砂岩的力学参数及可压裂性指 数对比

对比2种沉积微相砂岩的脆性指数和抗压强度(图9):水下分流河道砂岩的脆性指数分布在0~0.6,分布较均匀,席状砂的脆性指数分布在0.2~0.8,分布更为集中(图9a);水下分流河道砂岩

的抗压强度多分布在210~225,席状砂的抗压强度多分布在225~255,席状砂的抗压强度明显高于分流河道(图9b)。对研究区长7段的沉积微相和上述实验获得的可压裂性参数进行对比,整体上席状砂的可压裂性指数要高于水下分流河道砂岩,水下分流河道砂岩的可压裂性指数多集中在0.2~2.6,席状砂的可压裂性指数则分布于1.0~3.4(图9c)。

### 5.2 影响不同沉积微相砂岩可压裂性的主控因素 分析

为判断致密砂岩成分和结构各参数对可压裂性的影响强弱程度,参考已有研究方法(龙章亮等,2020),利用灰色关联法对各参数与可压裂性进行分析。

根据灰色关联法得到各参数与可压裂性的关联度,所得数值越大表明该影响因素对指标的影响越大,以此判断出各参数影响可压裂性的程度,分析结果见图10。

前文对砂岩成分结构与可压裂性的分析已经表明:碳酸盐矿物含量、石英含量、粒度分布标准偏差与可压裂性指数成正相关关系,即碳酸盐矿物与石英含量越高、标准偏差越大(分选越差),可压裂性越好;平均粒径以及长石含量与可压裂性指数

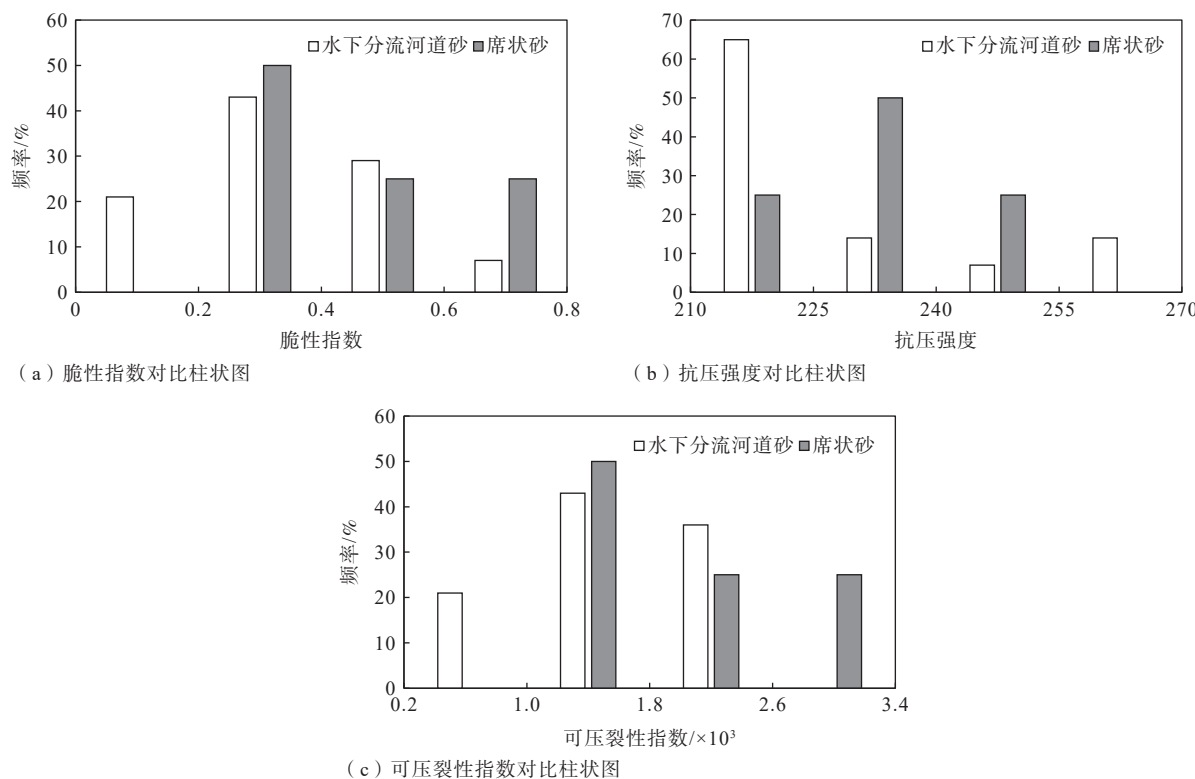


图9 不同沉积微相砂岩的可压裂性参数对比图

Fig. 9 Comparison of fracturability parameters for different sedimentary microfacies

(a) Brittleness index comparison bar chart; (b) Compressive strength comparison bar chart; (c) Fracability index comparison bar chart

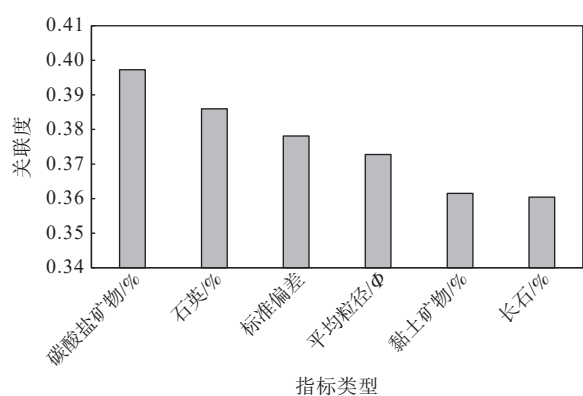


图 10 砂岩成分和结构参数与可压裂性指数的关联度

Fig. 10 The correlation between component or structure parameters and fracability index

成弱负相关关系,即粒度越细,长石含量越高,可压裂性趋于变差。

从灰色关联分析结果可以看出(图 10),砂岩各项参数对可压裂性影响的程度从高到低,可以按照碳酸盐矿物含量、石英含量、标准偏差、平均粒径的顺序排列,而黏土矿物和长石含量 2 个参数则处于影响相对较弱的位置。

席状砂与水下分流河道砂岩相比,石英含量相差不大,但碳酸盐矿物含量更高、分选性更差。尽管席状砂的粒度略偏细,但其平均粒径对可压裂性的影响程度处于相对次要位置,故而席状砂整体表现出更好的可压裂性。

## 6 结论

(1)鄂尔多斯盆地陇东地区长 7 段主要发育水下分流河道和席状砂 2 种沉积微相,水下分流河道的单砂体厚度大于 2 m,席状砂多为中厚层砂岩和泥岩互层,单砂体厚度一般小于 2 m。

(2)由于沉积和成岩特征的差异,水下分流河道和席状砂微相的砂岩在成分和结构上具有明显不同:席状砂中碳酸盐矿物、黏土矿物与杂基含量相对较高,粒度偏细,分选更差。这些不同是造成致密砂岩可压裂性差异的主要内在因素,也是依据沉积微相来判断致密砂岩可压裂性的根本。

(3)砂岩的可压裂性指数与其成分和结构具有相关性。在成分方面,可压裂性指数与石英矿物含量、碳酸盐矿物含量表现正相关性,与长石矿物含量呈现负相关性;在结构方面,可压裂性指数与平

均粒径表现为负相关关系,粒径越大,可压裂性指数越高;可压裂性指数与粒度分布标准偏差呈正相关关系,表明颗粒分选越差,可压裂性指数越高。

(4)通过灰色关联分析发现,砂岩的碳酸盐矿物含量、分选性和粒径对致密砂岩可压裂性的影响起主要作用。相对于水下分流河道微相,席状砂的分选性较差且碳酸盐矿物含量多,导致其具有更好的可压裂性。

## References

- BAI M, 2016. Why are brittleness and fracability not equivalent in designing hydraulic fracturing in tight shale gas reservoirs[J]. *Petroleum*, 2(1): 1-19.
- CAO Y, LIU Y Z, DUAN X T, et al., 2018. Sedimentary geological significance of reservoir in the lower Member of Yanchang Formation in Dingbian Area[J]. *Journal of Xi'an University of Science and Technology*, 38(1): 137-144. (in Chinese with English abstract)
- ESTUPIÑAN J, MARFIL R, DELGADO A, et al., 2007. The impact of carbonate cements on the reservoir quality in the Napo Fm sandstones (Cretaceous Oriente Basin, Ecuador)[J]. *Geologica Acta*, 5(1): 89-108.
- FAN H, ZHANG S, GOU X P, et al., 2011. A new numerical calibration of the critical stress intensity factor for the CCNBD specimens used in rock fracture toughness test[J]. *Chinese Journal of Applied Mechanics*, 28(4): 416-422. (in Chinese with English abstract)
- FOWELL R J, 1995. Suggested method for determining mode I fracture toughness using cracked chevron notched Brazilian disc (CCNBD) specimens[J]. *International Journal of Rock Mechanics and Mining Sciences & Geomechanics Abstracts*, 32(1): 57-64.
- Frankie M A, Mohd K A K, Mohd E T, et al., 2016. Sediment Classification using Envirometric Technique: A Study Case in Pahang River, Malaysia[J]. *The Malaysian Journal of Analytical Sciences*, 20 (5): 1171-1180.
- FU J H, LUO S S, NIU X B, et al., 2015. Sedimentary characteristics of channel Type Gravity Flow of the member 7 of Yanchang Formation in the Longdong area, Ordos Basin[J]. *Bulletin of Mineralogy, Petrology and Geochemistry*, 34(1): 29-37. (in Chinese with English abstract)
- FU J H, WANG X Z, ZHANG L X, 2015. Geological controls on artificial fracture networks in continental shale and its fracability evaluation: a case study in the Yanchang Formation, Ordos Basin, China[J]. *Journal of Natural Gas Science and Engineering*, 26: 1285-1293.
- HE R, YANG Z Z, LI X G, et al., 2019. A comprehensive approach for fracability evaluation in naturally fractured sandstone reservoirs based on analytical hierarchy process method[J]. *Energy Science & Engineering*, 7(2): 529-545.
- HOLT R M, FJÆR E, STENEBRÅTEN J F, et al., 2015. Brittleness of shales: relevance to borehole collapse and hydraulic fracturing[J]. *Journal of Petroleum Science and Engineering*, 131: 200-209.

- JIA X M, WANG Q Z, 2003. Wide range calibration of the stress intensity factor for the fracture toughness specimen CCNBD[J]. *Rock and Soil Mechanics*, 24(6): 907-912. (in Chinese with English abstract)
- JIN X C, SHAH S N, ROEGIERS J C, et al., 2015. An integrated petrophysics and geomechanics approach for fracability evaluation in shale reservoirs[J]. *SPE Journal*, 20(3): 518-526.
- KIVI I R, AMERI M, MOLLADAVOODI H, 2018. Shale brittleness evaluation based on energy balance analysis of stress-strain curves[J]. *Journal of Petroleum Science and Engineering*, 167: 1-19.
- LI J B, LU S F, CHEN G H, et al., 2015. Friability evaluation for the mud shale reservoirs based on the mineralogy and rock mechanics[J]. *Petroleum Geology and Oilfield Development in Daqing*, 34(6): 159-164. (in Chinese with English abstract)
- LI N Y, DAI J X, LIU C, et al., 2016. Feasibility research on volume acid fracturing to tight carbonate gas reservoir and its construction effect: a case study of lower Paleozoic carbonate gas reservoir in Ordos Basin[J]. *Petroleum Geology and Recovery Efficiency*, 23(3): 120-126. (in Chinese with English abstract)
- LI X B, LIU H Q, CHEN Q L, et al., 2010. Characteristics of slope break Belt in large Depression lacustrine basin and its controlling effect on Sandbody and petroleum: taking the Triassic Yanchang Formation in the Ordos Basin as an example[J]. *Acta Sedimentologica Sinica*, 28(4): 717-729. (in Chinese with English abstract)
- LI Z Y, FAN M M, MA Y, et al., 2012. Depositional facies of Chang 7 oil formation of the Triassic Yanchang formation in southeast Ordos Basin[J]. *Journal of Shaanxi University of Science & Technology*, 30(1): 106-110+121. (in Chinese with English abstract)
- LIAO J J, ZHU X M, DENG X Q, et al., 2013. Sedimentary characteristics and model of gravity flow in Triassic Yanchang Formation of Longdong area in Ordos Basin[J]. *Earth Science Frontiers*, 20(2): 29-39. (in Chinese with English abstract)
- LIU F, ZHU X M, LI Y, et al., 2015. Sedimentary characteristics and facies model of gravity flow deposits of Late Triassic Yanchang Formation in southwestern Ordos Basin, NW China[J]. *Petroleum Exploration and Development*, 42(5): 577-588. (in Chinese with English abstract)
- LIU J, HUI C, FAN J M, et al., 2021. Distribution characteristics of the present-day in-situ stress in the Chang 6 tight sandstone reservoirs of the Yanchang Formation in the Heshui Area, Ordos Basin, China and suggestions for development[J]. *Journal of Geomechanics*, 27(1): 31-39. (in Chinese with English abstract)
- LIU L Q, LI Y, KANG L M, et al., 2010. Mudstone distribution features of maximum flooding time in late Triassic in Ordos Basin[J]. *Journal of Northwest University (Natural Science Edition)*, 40(5): 866-871. (in Chinese with English abstract)
- LONG Z L, WEN Z T, LI H, et al., 2020. An evaluation method of shale reservoir crushability based on grey correlation analysis[J]. *Reservoir Evaluation and Development*, 10(1): 37-42. (in Chinese with English abstract)
- MU L J, ZHAO Z F, LI X W, et al., 2019. Fracturing technology of stimulated reservoir volume with subdivision cutting for shale oil horizontal wells in Ordos Basin[J]. *Oil & Gas Geology*, 40(3): 626-635. (in Chinese with English abstract)
- REN Y, CAO H, YAO F C, et al., 2018. Brittleness and fracability prediction for tight oil reservoir in Jimsar Sag, Junggar Basin[J]. *Oil Geophysical Prospecting*, 53(3): 511-519. (in Chinese with English abstract)
- RICKMAN R, MULLEN M, PETRE E, et al., 2008. A practical use of shale petrophysics for stimulation design optimization: all shale plays are not clones of the Barnett Shale[C]//SPE annual technical conference and exhibition. Denver: SPE: 21-24.
- SUN Y, JIANG Y Q, XIONG X Y, et al., 2022. Lithofacies and sedimentary environment evolution of the Shan2 3 Sub-member transitional shale of the Shanxi Formation in the Daning-Jixian area, eastern Ordos Basin[J]. *Coal Geology & Exploration*, 50(9): 104-114. (in Chinese with English abstract)
- SUI L L, JU Y, YANG Y M, et al., 2016. A quantification method for shale fracability based on analytic hierarchy process[J]. *Energy*, 115: 637-645.
- WANG D B, GE H K, WANG X Q, et al., 2015. A novel experimental approach for fracability evaluation in tight-gas reservoirs[J]. *Journal of Natural Gas Science and Engineering*, 23: 239-249.
- WANG Q Z, 1998. Stress intensity factors of the ISRM suggested CCNBD specimen used for mode-I fracture toughness determination[J]. *International Journal of Rock Mechanics and Mining Sciences*, 35(7): 977-982.
- WU J J, ZHANG S H, CAO H, et al., 2018. Fracability evaluation of shale gas reservoir-A case study in the Lower Cambrian Niutitang formation, northwestern Hunan, China[J]. *Journal of Petroleum Science and Engineering*, 164: 675-684.
- YANG F, MEI W B, LI L, et al., 2023. Propagation of hydraulic fractures in thin interbedded tight sandstones[J]. *Coal Geology & Exploration*, 51(7): 61-71. (in Chinese with English abstract)
- YANG H, DOU W T, LIU X Y, et al., 2010. Analysis on sedimentary facies of Member 7 in Yanchang formation of Triassic in Ordos Basin[J]. *Acta Sedimentologica Sinica*, 28(2): 254-263. (in Chinese with English abstract)
- YAO J L, DENG X Q, ZHAO Y D, et al., 2013. Characteristics of Tight oil in triassic Yanchang Formation, Ordos Basin[J]. *Petroleum Exploration and Development*, 40(2): 150-158. (in Chinese with English abstract)
- YUAN J L, DENG J G, ZHANG D Y, et al., 2013. Fracability evaluation of shale-gas reservoirs[J]. *Acta Petrolei Sinica*, 34(3): 523-527. (in Chinese with English abstract)
- ZHANG H L, DENG N T, ZHANG Z H, et al., 2014. Geochemical characteristics and oil-source correlation of the Mesozoic Crude Oils in the Southern Ordos Basin[J]. *Geological Journal of China Universities*, 20(2): 309-316. (in Chinese with English abstract)
- ZHANG X H, FENG S Y, LIANG X W, et al., 2020. Sedimentary microfacies identification and inferred evolution of the Chang 7 member of Yanchang Formation in the Longdong area, Ordos Basin[J]. *Acta Geologica Sinica*, 94(3): 957-967. (in Chinese with English abstract)
- ZHANG Z H, WEI X S, GONG H J, et al., 2020. Diagenesis characteristics

- and evolution of porosity of Chang7 tight sandstone reservoir in Dingbi-an oilfield, Ordos Basin[J]. Petroleum Geology and Recovery Efficiency, 27(2): 43-52. (in Chinese with English abstract)
- ZHAO J Y, JI D S, WU J, et al., 2022. Research on rock mechanics parameters of the Jurassic-Cretaceous reservoir in the Sikeshu sag, Junggar Basin, China[J]. Journal of Geomechanics, 28(4): 573-582. (in Chinese with English abstract)
- ZHONG D K, ZHU X M, LI S J, et al., 2007. Influence of early carbonate cementation on the evolution of sandstones: a case study from Silurian sandstones of Manjiaer depression, Tarim basin[J]. Acta Sedimentologica Sinica, 25(6): 885-890. (in Chinese with English abstract)
- TANG S H, LUO Y S, ZHOU Z B, 2008. Plastic variational principle based on the least work consumption principle[J]. Journal of Central South University of Technology, 15(S1): 39-42.
- ZOU C N, ZHAO Z Z, YANG H, et al., 2009. Genetic mechanism and Distribution of sandy Debris flows in Terrestrial lacustrine basin[J]. Acta Sedimentologica Sinica, 27(6): 1065-1075. (in Chinese with English abstract)
- ZOU C N, YANG Z, ZHANG G S, et al., 2014. Conventional and unconventional petroleum "Orderly accumulation": concept and practical significance[J]. Petroleum Exploration and Development, 41(1): 14-27. (in Chinese with English abstract)
- 110+121.
- 廖纪佳, 朱筱敏, 邓秀芹, 等, 2013. 鄂尔多斯盆地陇东地区延长组重力流沉积特征及其模式[J]. 地学前缘, 20(2): 29-39.
- 刘芬, 朱筱敏, 李洋, 等, 2015. 鄂尔多斯盆地西南部延长组重力流沉积特征及相模式[J]. 石油勘探与开发, 42(5): 577-588.
- 刘建, 惠晨, 樊建明, 等, 2021. 鄂尔多斯盆地合水地区长6致密砂岩储层现今地应力分布特征及其开发建议[J]. 地质力学学报, 27(1): 31-39.
- 刘联群, 李勇, 康立明, 等, 2010. 鄂尔多斯盆地晚三叠世最大湖泛泥岩分布特征[J]. 西北大学学报(自然科学版), 40(5): 866-871.
- 龙章亮, 温真桃, 李辉, 等, 2020. 一种基于灰色关联分析的页岩储层可压性评价方法[J]. 油气藏评价与开发, 10(1): 37-42.
- 慕立俊, 赵振峰, 李宪文, 等, 2019. 鄂尔多斯盆地页岩油水平井细切割体积压裂技术[J]. 石油与天然气地质, 40(3): 626-635.
- 孙越, 蒋裕强, 熊先锐, 等, 2022. 鄂尔多斯盆地东缘大宁-吉县地区山西组山23亚段海陆过渡相页岩岩相与沉积环境变化[J]. 煤田地质与勘探, 50(9): 104-114.
- 杨帆, 梅文博, 李亮, 等, 2023. 薄互层致密砂岩水力压裂裂缝扩展特征研究[J]. 煤田地质与勘探, 51(7): 61-71.
- 杨华, 窦伟坦, 刘显阳, 等, 2010. 鄂尔多斯盆地三叠系延长组长7沉积相分析[J]. 沉积学报, 28(2): 254-263.
- 姚泾利, 邓秀芹, 赵彦德, 等, 2013. 鄂尔多斯盆地延长组致密油特征[J]. 石油勘探与开发, 40(2): 150-158.
- 袁俊亮, 邓金根, 张定宇, 等, 2013. 页岩气储层可压裂性评价技术[J]. 石油学报, 34(3): 523-527.
- 张海林, 邓南涛, 张枝焕, 等, 2014. 鄂尔多斯盆地南部中生界原油地球化学特征及油源分析[J]. 高校地质学报, 20(2): 309-316.
- 张晓辉, 冯顺彦, 梁晓伟, 等, 2020. 鄂尔多斯盆地陇东地区延长组7段沉积微相及沉积演化特征[J]. 地质学报, 94(3): 957-967.
- 张哲豪, 魏新善, 弓虎军, 等, 2020. 鄂尔多斯盆地定边油田长7致密砂岩储层成岩作用及孔隙演化规律[J]. 油气地质与采收率, 27(2): 43-52.
- 赵进雍, 冀冬生, 吴见, 等, 2022. 准噶尔盆地四棵树凹陷侏罗系—白垩系储层岩石力学参数研究[J]. 地质力学学报, 28(4): 573-582.
- 钟大康, 朱筱敏, 李树静, 等, 2007. 早期碳酸盐胶结作用对砂岩孔隙演化的影响: 以塔里木盆地满加尔凹陷志留系砂岩为例[J]. 沉积学报, 25(6): 885-890.
- 邹才能, 赵政璋, 杨华, 等, 2009. 陆相湖盆深水砂质碎屑流成因机制与分布特征: 以鄂尔多斯盆地为例[J]. 沉积学报, 27(6): 1065-1075.
- 邹才能, 杨智, 张国生, 等, 2014. 常规-非常规油气“有序聚集”理论认识及实践意义[J]. 石油勘探与开发, 41(1): 14-27.

## 附中文参考文献

- 曹跃, 刘延哲, 段昕婷, 等, 2018. 定边地区延长组下部储层的沉积地质意义[J]. 西安科技大学学报, 38(1): 137-144.
- 樊鸿, 张盛, 苟小平, 等, 2011. 岩石断裂韧度试样CCNBD临界应力强度因子的全新数值标定[J]. 应用力学学报, 28(4): 416-422.
- 付金华, 罗顺社, 牛小兵, 等, 2015. 鄂尔多斯盆地陇东地区长7段沟道型重力流沉积特征研究[J]. 矿物岩石地球化学通报, 34(1): 29-37.
- 贾学明, 王启智, 2003. 断裂韧度试样CCNBD宽范围应力强度因子标定[J]. 岩土力学, 24(6): 907-912.
- 李进步, 卢双舫, 陈国辉, 等, 2015. 基于矿物学和岩石力学的泥页岩储层可压裂性评价[J]. 大庆石油地质与开发, 34(6): 159-164.
- 李年银, 代金鑫, 刘超, 等, 2016. 致密碳酸盐岩气藏体积酸压可行性研究及施工效果: 以鄂尔多斯盆地下古生界碳酸盐岩气藏为例[J]. 油气地质与采收率, 23(3): 120-126.
- 李相博, 刘化清, 陈启林, 等, 2010. 大型坳陷湖盆沉积坡带折带特征及其对砂体与油气的控制作用: 以鄂尔多斯盆地三叠系延长组为例[J]. 沉积学报, 28(4): 717-729.
- 李兆扬, 范萌萌, 马遥, 等, 2012. 鄂尔多斯盆地东南部长7油层组沉积相研究[J]. 陕西科技大学学报(自然科学版), 30(01): 106-